

- [8] R. M. Haralick, L. T. Watson, and T. J. Laffey, "The topographic primal sketch," *Int. J. Robot. Res.*, vol. 2, pp. 50-72, 1983.
- [9] L. R. Nackman, "Two-dimensional critical point configuration graphs," *IEEE Trans. Pattern Anal. Machine Intell.*, vol. PAMI-6, pp. 442-450, July 1984.
- [10] L. Dreschler, "Zur Reproduzierbarkeit von markanten Bildpunkten bei der Auswertung von Realwelt-Bildfolgen," in *Modelle und Strukturen: DAGM Symp.*, Hamburg, West Germany, Oct. 1981, Springer-Verlag Inf. Fachber. V.49, pp. 76-82.
- [11] J. Dengler and J. Bille, "A scene analysis system simulating the peripheral visual perception," in *Proc. 7th Int. Conf. Pattern Recogn.*, Montreal, P.Q., Canada, July 1984, pp. 863-865.
- [12] A. Rosenfeld, Y. H. Lee, and R. B. Thomas, "Edge and curve detection for texture discrimination," in *Picture Processing and Psychopictorics*, B. S. Lipkin and A. Rosenfeld Eds. New York: Academic, 1970.
- [13] R. Harris, and E. C. Barrett, "Toward an objective nephanalysis," *J. Appl. Meteorol.*, vol. 17, pp. 1258-1266, 1978.
- [14] R. Fisher, "Dispersion on a sphere," in *Proc. Roy. Soc. London*, A217, pp. 295-305, 1953.
- [15] R. M. Haralick and L. Watson, "A facet model for image data," *Comput. Graph. Image Processing*, vol. 15, pp. 113-129, 1981.
- [16] R. M. Haralick, "Statistical and structural approaches to texture," *Proc. IEEE*, vol. 67, pp. 786-804, May 1979.
- [17] A. Rosenfeld and A. C. Kak, *Digital Picture Processing*. 2nd ed., vol. 2. New York: Academic, 1982.
- [18] E. L. Hall, *Computer Image Processing and Recognition*. New York: Academic, 1979.
- [19] W. K. Pratt, *Digital Image Processing*. New York: Wiley, 1978.
- [20] F. G. Peet and T. S. Sahota, "A computer-assisted cell identification system," *Anal. Quantit. Cytol.*, vol. 6, pp. 59-70, Mar. 1984.
- [21] P. H. Bartels and G. B. Olson, "Computer analysis of lymphocyte images," in *Methods of Cell Separation*, vol. 3, N. Catsimopoulos, Ed. New York: Plenum, 1980.
- [22] H. Genchi and K. Mori, "Evaluation and feature extraction on automatic pattern recognition system," *Denkin-Tsushin Gakkai, Part I*, 1965 (in Japanese). Quoted in N. Tanaka *et al.*, "Fundamental study of automatic cyto-screening for uterine cancer: I. Feature evaluation for the pattern recognition system," *Acta. Cytol.*, vol. 21, pp. 72-78, 1977.
- [23] E. M. Sherwood, P. H. Bartels, and G. L. Wied, "Feature selection in cell image analysis: Use of the ROC curve," *Acta. Cytol.*, vol. 20, pp. 255-261, 1976.
- [24] B. de Campos Vidal, G. Schluter, and G. W. Moore, "Cell nucleus pattern recognition: Influence of staining," *Acta. Cytol.*, vol. 17, pp. 510-521, 1973.

Description and Discrimination of Planar Shapes Using Shape Matrices

ARDESHIR GOSHTASBY

Abstract—A shape descriptor has been developed which can describe a shape independent of its translation, rotation, and scaling. The description is in the form of a matrix and it is obtained by a polar quantization of a shape. The quantization process takes into consideration not only a shape's outer geometry but its inner geometry as well. The descriptor is information preserving and if the quantization parameters are selected properly, it is possible to reconstruct an original shape from its description. In this technique, shape discrimination is possible by a simple EXCLUSIVE-OR operation on shape descriptions.

Index Terms—Information-preserving description, object-centered description, shape discrimination, shape matrix, template matching.

Manuscript received October 17, 1983; revised May 15, 1985. Recommended for acceptance by S. L. Tanimoto.

The author is with the Department of Computer Science, University of Kentucky, Lexington, KY 40506.

I. INTRODUCTION

Description and discrimination of planar shapes is one of the fundamental problems in computer vision and pattern recognition. To discriminate shapes, a procedure to describe them is usually required. Then, by comparing shape descriptions, shape discrimination is achieved.

There are various measures for describing a shape. Some measures use distances such as the ratio of the length of the longest side and the perimeter of the shape, the standard deviation of the length of the sides of the shape, and the length of the perimeter and the derivatives of its side lengths [16]. Some measures use angles such as the ratio of the largest to the smallest angle, the ratio of the largest angle to the total degree of angles, and the standard deviation of angles [16].

Moments of side lengths, radii, and angles are used to describe shapes too. In [2], the first four moments of the angles given by

$$M_k = \sum_{i=1}^n (a_i - \bar{a})^k / n$$

are used to describe shapes. In this formula, k is the power of the moment, n is the number of angles, a_i is the size of angle i , and \bar{a} is the mean of the angle. Similar formulas can be used to compute the moments of side lengths and radii.

A measure which describes the degree of compactness of a shape is P^2/A where P and A are the perimeter and area of the shape, respectively [16]. Given different shapes of a constant area, the one with the smallest perimeter is the most compact shape.

Other measures which are used for shape description are measures of regularity [16] and angular variability [1]. Regularity is defined as the ratio of the standard deviation of side lengths and standard deviation of all angles. Angular variability is the mean absolute difference of adjacent angles taken in overlapping pairs about the boundary where convex angles are given a positive sign and concave angles are given a negative sign.

A description which is obtained by polar quantization of a shape is described in [12]. In this description, the shape contour is sampled with equal angular steps relative to the center of gravity of the shape. Then, distances of the sample points to the center of gravity of the shape are plotted as a function of their angles. The obtained waveform has been called the signature of the shape. If, at a given angle, the contour is intersected at more than one point, the largest distance or the sum of the distances is used as the distance value for the angle.

The shape measures (descriptors) that were given above are not information preserving because it is not possible to reconstruct the original shapes using their descriptions. A large number of shapes may have the same description. There are descriptors, however, that are information preserving and uniquely represent a shape. Some of the information-preserving descriptors are: invariant moments [8], Fourier descriptors [13], [15], and centroidal profiles [5].

Freeman's centroidal profile is similar to the Peli's shape signature except that instead of taking sample points at equal angular steps, the sample points are taken at equal distances on the shape contour. In the centroidal profile, since each point on the shape corresponds to a unique point on the profile, the representation is unique and information preserving.

By traveling along a closed boundary repeatedly, the centroidal profile is repeated also creating a periodic function. Fourier descriptors express a centroidal profile by Fourier series and use the obtained Fourier coefficients to characterize a shape.

Another information-preserving shape descriptor is the invariant moments developed by Hu [8]. In this technique, coordinates of points belonging to the shape are used to compute a set of moments. Then, the moments are normalized to obtain measures that are invariant under translation, rotation, and scaling of the shape. In [4], invariant moments have been used to identify aircraft shape boundaries.

Most techniques for shape description use shape boundaries and the patterns inside the shape are forgotten. In many instances (such as industrial parts, chinese characters, etc.), information about internal geometry of a shape considerably enhances the shape discrimination process. In the following, a shape descriptor which takes into consideration the shape's internal geometry as well as its external geometry is described.

II. SHAPE DESCRIPTION

In this section, a shape is transformed into a matrix by polar quantization of the shape. Assuming O is the center of gravity of the shape and OA with length L is the maximum radius of the shape, to obtain an $m \times n$ matrix representation of the shape, we divide OA into $n - 1$ equal distances and draw circles centering at O and radii $L/(n - 1), 2L/(n - 1), \dots, (n - 1)L/(n - 1)$, see Fig. 1(a). If the circles intersect the maximum radius of the shape (line OA) at i_1, i_2, \dots, i_{n-1} , then starting from i_1, i_2, \dots, i_{n-1} and counter-clockwise, we divide each circle into m equal arcs, each arc being $d\theta = 360/m$ degrees. Then an $m \times n$ matrix is constructed according to the following algorithm. This matrix will be called the "shape matrix."

Algorithm 1: Construction of a shape matrix of size $m \times n$ for a given shape.

1. Create an $m \times n$ matrix and call it M
2. For $i = 0$ to $n - 1$
3. For $j = 0$ to $m - 1$
4. If the point with polar coordinates $(iL/(n - 1), j(360/m))$ lies inside the shape, then let $M(i, j) = 1$,
 otherwise let $M(i, j) = 0$.

The shape matrix of Fig. 1(a) for $m = 6$ and $n = 5$ is shown in Fig. 1(b). Note that when implementing the shape matrix, information was gathered in an object-centered coordinate system that was normalized with respect to the maximum radius of the shape. The obtained shape matrix is invariant of translation, rotation, and scaling of the shape.

If the shape does not have any holes and each radial axis intersects the shape at only one point, then the shape signature of Peli [12] is similar to the boundary between the 0's and 1's in the shape matrix. However, when the shape has holes or if some radial axes intersect the shape at more than one point, then shape signature and boundary of 0's and 1's in the shape matrix would be different. Fig. 2 shows a shape of the first kind and Fig. 3 shows a shape of the second kind with their shape matrices and signatures.

Representing a shape in matrix form has many nice properties. In Section III, some of the properties of shape matrices are discussed.

III. PROPERTIES OF SHAPE MATRICES

Marr and Nishihara [9] have proposed three criteria for judging the effectiveness of a shape descriptor. These are accessibility, scope and uniqueness, and stability and sensitivity. In the following, these criteria will be used to evaluate the effectiveness of shape matrices as shape descriptors.

A. Accessibility

Accessibility tells how economically (in terms of computation time and memory usage) a descriptor can be generated from a shape in digital images. To implement a shape matrix of size $m \times n$ for a given shape, algorithm 1 requires mn operations. Each operation being two multiplications and a memory lookup. The memory requirements for the shape matrix is $m \times n$ bits. How large are m and n ?

If there are L pixels on the maximum radius of the shape, it would not make sense to let $n > L$ because then we would be quantizing the shape with steps smaller than a pixel and this would only bring repeated information. Therefore, $n \leq L$. Assuming a complete solid circular shape of radius L , there will be $2\pi L$ pixels on the perimeter of the shape and again quantizing the shape by angular steps smaller than $d\theta = 360/2\pi L$ degrees would not make

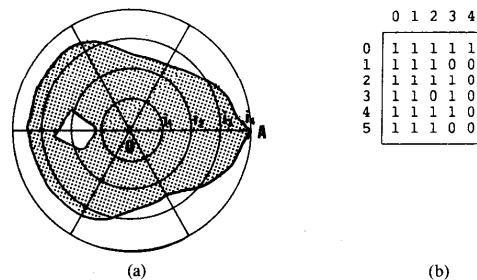


Fig. 1. (a) A shape and (b) its shape matrix.

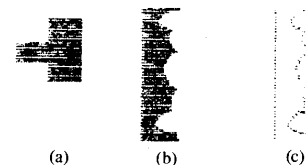


Fig. 2. (a) A shape with no hole and no radial axis intersecting the shape at more than one point. (b) Shape matrix. (c) Shape signature.

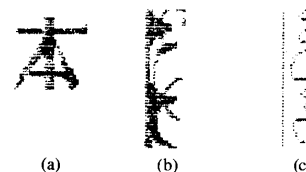


Fig. 3. (a) A shape with holes and some radial axes intersecting the shape at more than one point. (b) Shape matrix. (c) Shape signature.

sense because more than one radial axis will be passed through pixels even on the boundary of a circle. Therefore, $n \leq 360/d\theta = 2\pi L$.

To compare the memory requirements of shape matrices and shape signatures, let us assume that a measurement can be stored in 16 bits of memory. Then for shapes with maximum radius $L \leq 16$, a shape matrix would require less or equal amounts of memory than a shape signature. Because the number of angular sample points is equal to the number of rows in the shape matrix, and we require 16 bits of memory to store the value of each sample point in the shape signature, while each row of the shape matrix, in this case, will be at most 16 bits memory. However, as the size of a shape increases, a shape signature would require less memory than a shape matrix to represent the shape.

B. Scope and Uniqueness

Scope shows the class of shapes that can be described by the descriptor, and uniqueness tells whether a description uniquely describes a shape or it represents a wide range of shapes. Shape matrices can represent any digital shape with no restrictions and, therefore, scope of shape matrices involve all planar shape patterns. If m and n are selected large enough ($m \geq 2\pi L$ and $n \geq L$), and the shape has only one maximum radius, then the representation is unique and the original shape can be reconstructed from its shape matrix. If a shape has many maximum radii, we can obtain as many descriptions as there are maximum radii in the shape. However, in this case as well, each description uniquely describes the shape, and from any of the descriptions we can obtain the original shape back.

To show the uniqueness of shape matrices, first, an algorithm which reconstructs a shape from its shape matrix is given. Then, it is proven that the obtained shape is the same as the original one.

Algorithm 2: Reconstruction of a shape from its shape matrix M of size $m \times n$.

1. Generate a grid with $(2n - 1) \times (2n - 1)$ cells, call it G
2. Assuming a Cartesian coordinate system at the center of the grid, as shown in Fig. 4, then
For $x = -(n - 1)$ to $(n - 1)$
3. For $y = -(n - 1)$ to $(n - 1)$
4. Compute $i = \tan^{-1}(y/x)/d\theta$ where $d\theta = 360/m$.
5. Compute $j = \text{sqrt}(x^2 + y^2)$.
6. If $j > n - 1$ then let $G(x, y) = 0$ otherwise
 let $G(x, y) = M(i, j)$.

Fig. 4 shows reconstruction of Fig. 1(a) by applying algorithm 2 on the shape matrix of Fig. 1(b).

Proposition 1: If the values of m and n are selected properly ($m \geq 2\pi L$ and $n > L$), then a shape matrix that has been obtained by algorithm 1 can be used to reconstruct the original shape using algorithm 2. In the following, an element of the original shape is referred to as a pixel, an element of the shape matrix is referred to as an element, and an element of the grid produced by algorithm 2 is referred to as a cell. L is the number of pixels on the maximum radius of the shape.

Proof: A pixel which belongs to the shape at distance $d \leq L$ from the center of gravity of the shape can be viewed from the center of gravity of the shape by angle $d\theta' = 360/2\pi d \geq 360/2\pi L$. Now, if we let $m \geq 2\pi L$ and $n \geq L$, then two neighboring elements in a column of the shape matrix differ by $d\theta = 360/m \leq 360/2\pi L \leq d\theta'$ and two neighboring elements in a row of the shape matrix differ by $L/n \leq 1$ units. This shows that each pixel in the shape is mapped to at least one element in the shape matrix by algorithm 1.

Also, since a cell at distance $d' \leq L$ from the center of the grid is viewed from the center of the grid by angle $d\theta'' = 360/2\pi d' \geq 360/m = d\theta$, then in algorithm 2, a cell in the grid also corresponds to at least one element in the shape matrix. This shows that each element of the grid is marked at least once by algorithm 2.

Now, if element (i, j) of the matrix is 1, the cell with coordinates (x, y) [such that the cell's distance to the center of the grid is $\text{sqrt}(x^2 + y^2)$ and its angle with respect to the x axis is $\tan^{-1}(y/x)$] will be marked as belonging to the shape by algorithm 2. We also know that element (i, j) of the shape matrix is set to 1 by algorithm 1 only if the pixel at distance $iL/(m - 1)$, from the center of gravity of the shape and angle $j(360/m)$ with the maximum radius of the shape, belongs to the shape. Since $i(360/m) = \tan^{-1}(y/x)$ and $jL/(n - 1) = \text{sqrt}(x^2 + y^2)$ with a scaling factor, $(L/(n - 1))$ is the unit of measurement of the original shape. Therefore, the reconstructed shape will have the same geometry as the original shape. We conclude that if a shape with maximum radius L is available and a shape matrix of size $m \geq 2\pi L$ and $n \geq L$ is constructed using algorithm 1, the original shape can be reconstructed from its shape matrix using algorithm 2.

C. Stability and Sensitivity

Stability tells how stable the description is in representing the general property of the shape, and sensitivity shows how sensitive the description is to finer distinctions between shapes. For a shape with maximum radius L , if we take the dimensions of the shape matrix $m \geq 2\pi L$ and $n \geq L$ then according to Section III-B, the description will be information preserving and it will provide all details in the shape, therefore enabling discrimination of shapes even with small differences. The amount of memory used to store this shape matrix is $2\pi L^2$ which is at least 2 times larger than the original shape. This is the cost to be paid in terms of memory to store an information-preserving description.

When a coarser sampling rate is applied ($m < 2\pi L$, $n < L$), such as shape signatures, shape matrices remain sensitive to small details in the shape which actually could be the noise. Therefore, when coarse sampling is required, it is advisable to smooth the shape first to remove the noise and then carry out the sampling.

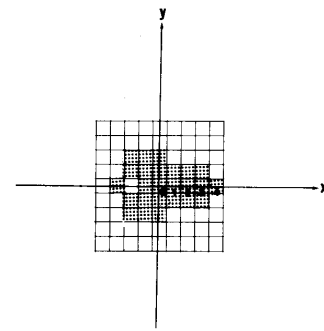


Fig. 4. Shape obtained by applying algorithm 2 on shape matrix of Fig. 1(b).

IV. SHAPE DISCRIMINATION

Since shape matrices describe shapes independent of their position, orientation, or scale, to discriminate shapes, we only need to compare their shape matrices. Because shape matrices are binary matrices, their comparison would involve only an EXCLUSIVE-OR (XOR) operation. The more similar two shape matrices are, the fewer the number of 1's in the obtained matrix. More specifically, the similarity between two shapes can be determined by the following algorithm.

Algorithm 3: Determination of similarity between two shapes with shape matrices $M1$ and $M2$ of size $m \times n$.

1. $S := 0$
2. For $i = 0$ to $m - 1$.
3. For $j = 0$ to $n - 1$
4. $S := S + M1(i, j) \cdot \text{XOR} \cdot M2(i, j)$
5. Similarity: $= 1 - S/(m - 2)n$.

Step 5 of algorithm 3 is adjusted so that when two shapes are completely similar ($S = 0$), we obtain similarity = 1. A circle and a line have been defined as two completely dissimilar shapes. A line corresponds to a shape matrix with two rows of 1's and a circle corresponds to a shape matrix with all elements equal to 1. Their difference is $S = (m - 2)n$, and similarity = 0 is obtained. Other shapes will produce similarities between 0.0 and 1.0.

It should be noted that algorithm 3 implicitly assumes that each shape has a unique maximum radius. If some shapes have more than one maximum radius, the matching should be carried out for the shape matrices obtained by each maximum radii. The matching that gives the highest similarity measure should be taken as the correct one. In noisy images where an artificial maximum radius could be obtained anywhere on the shape, a full cyclic rotation of one shape should be matched with the other shape.

The computational complexity of algorithm 3 is mn operations where each operation consists of an EXCLUSIVE-OR and an addition. Assuming the maximum radius of a shape is L pixels, using $m = 2\pi L$ and $n = L$, the computation time would be proportional to $2\pi L^2$. Note that the EXCLUSIVE-OR can be carried out word-by-word rather than bit-by-bit. If done so, less computation time would be needed.

If the shape signature had been used, the computation time would have consisted of the following.

- Time for cross correlating two shape signatures each with m sample points. This would take $m = 2\pi L$ multiplications.
- If the shapes have rotational differences, one of the signatures should be incrementally rotated and the above operation should be repeated m times. Therefore, the total computation time would be $4\pi^2 L^2$ multiplications.
- If the shapes have scaling differences too, it is required to estimate the scaling factor by minimizing the squared errors at each rotational increment which would be a multiplication factor to the above time complexity when discriminating shapes.

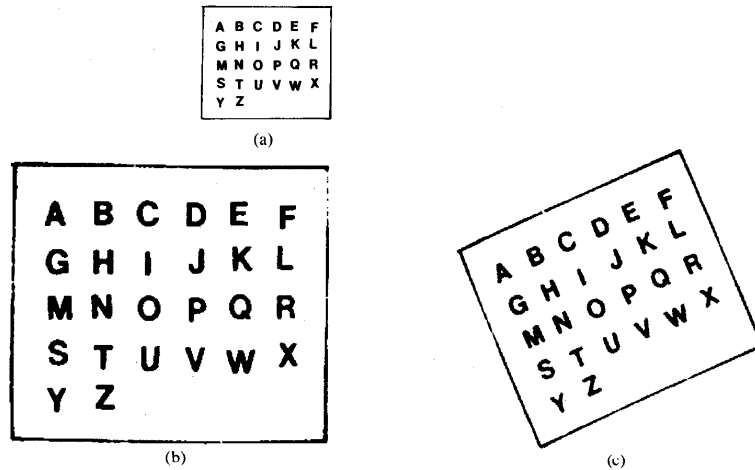


Fig. 7. (a) Original characters. (b) digitized. (c) rotated by 45°, slightly reduced in scale, and digitized again.

TABLE I
ALPHABET SHAPE SIMILARITIES OF FIG. 7(b) AND (c). THE BEST MATCHES ARE UNDERLINED

	A	B	C	D	E	F	G	H	I	J	K	L	M	N	O	P	Q	R	S	T	U	V	W	X	Y	Z	
A	<u>.90</u>	.54	.42	.42	.61	.73	.42	.59	.62	.63	.68	.63	.68	.61	.26	.73	.39	.66	.53	.62	.58	.78	.66	.67	.74	.54	A
B	.54	<u>.88</u>	.56	.63	.74	.63	.62	.79	.57	.55	.64	.58	.62	.70	.45	.53	.60	.70	.75	.63	.63	.65	.65	.60	.67	.67	B
C	.46	.57	<u>.88</u>	.77	.57	.46	.66	.47	.38	.56	.44	.56	.47	.46	.71	.65	.80	.55	.55	.47	.70	.56	.44	.40	.39	.54	C
D	.51	.61	<u>.76</u>	<u>.84</u>	.58	.49	.75	.53	.37	.57	.45	.56	.54	.53	.68	.61	.83	.62	.52	.50	.82	.60	.46	.40	.42	.49	D
E	.60	.66	.49	<u>.44</u>	<u>.94</u>	<u>.72</u>	.51	.60	.64	.73	.69	.67	.59	.67	.37	.59	.47	.60	.82	.70	.54	.60	.75	.65	.74	.70	E
F	.68	.59	.42	.43	<u>.76</u>	<u>.90</u>	.48	.66	.72	.80	.71	.69	.66	.67	.32	.74	.42	.74	.66	.70	.58	.66	.75	.75	.57	.57	F
G	.46	.67	.76	.76	.54	<u>.50</u>	<u>.85</u>	.58	.44	.57	.44	.55	.55	.55	.68	.55	.80	.62	.66	.48	.72	.54	.50	.43	.45	.63	G
H	.53	.82	.50	.60	.66	.65	<u>.58</u>	<u>.90</u>	.63	.60	.67	.63	.66	.79	.43	.51	.54	.72	.70	.70	.62	.58	.65	.74	.64	.70	H
I	.62	.59	.41	.39	.65	.72	.45	<u>.66</u>	<u>.91</u>	.75	.78	.75	.58	.74	.31	.51	.35	.61	.68	.82	.49	.56	.68	.80	.75	.77	I
J	.65	.49	.54	.55	.69	.77	.56	<u>.89</u>	<u>.71</u>	.94	.64	.79	.58	.60	.42	.71	.52	.75	.57	.70	.66	.68	.62	.66	.71	.62	J
K	.67	.61	.40	.40	.71	.74	.41	.67	.74	<u>.67</u>	<u>.89</u>	.69	.64	.72	.27	.58	.37	.67	.63	.72	.52	.60	.72	.82	.75	.65	K
L	.61	.54	.56	.54	.64	.65	.53	.65	.74	.78	.66	<u>.90</u>	.57	.64	.44	.64	.50	.72	.59	.74	.60	.63	.62	.68	.68	.69	L
M	.68	.66	.44	.51	.60	.68	.54	.73	.61	.64	.68	<u>.63</u>	<u>.82</u>	.68	.38	.66	.51	.70	.54	.58	.54	.66	.75	.68	.67	.60	M
N	.55	.69	.46	.54	.64	.61	.60	.79	.69	.59	.72	.58	.64	<u>.85</u>	.39	.55	.52	.70	.66	.69	.55	.65	.68	.61	.70	.70	N
O	.30	.51	.81	.77	.38	.29	.75	.42	.29	.43	.27	.45	.42	<u>.38</u>	<u>.90</u>	.38	.79	.42	.51	.34	.60	.39	.32	.29	.27	.49	O
P	.76	.50	.51	.53	.62	.78	.54	.84	.83	.73	.61	.66	.64	.69	<u>.97</u>	<u>.90</u>	.51	.73	.53	.60	.03	.77	.65	.62	.66	.46	P
Q	.42	.58	.80	.84	.46	.43	.75	.51	.39	.53	.36	.52	.51	.49	.77	.54	.90	.58	.51	.41	.74	.54	.45	.40	.37	.46	Q
R	.67	.65	.52	.57	.72	.76	.55	.69	.60	.72	.71	.71	.62	.73	.39	.74	.51	.90	.66	.68	.72	.70	.66	.66	.66	.55	R
S	.46	.78	.57	.55	.70	.55	.67	.70	.68	.59	.67	.54	.54	.66	.56	.43	.53	.61	.85	.67	.54	.48	.58	.62	.59	.63	S
T	.59	.63	.45	.43	.71	.70	.49	.73	.81	.68	.73	.75	.56	.69	.29	.56	.44	.64	.64	.89	.61	.65	.67	.74	.79	.73	T
U	.67	.56	.68	.73	.60	.60	.63	.59	.49	.60	.56	.62	.56	.61	.53	.74	.70	.72	.57	.56	.87	.48	.50	.49	.49	.49	U
V	.81	.59	.52	.54	.60	.66	.51	.54	.57	.66	.62	.69	.67	.56	.39	.75	.53	.63	.58	.60	.72	<u>.85</u>	.58	.58	.74	.47	V
W	.63	.60	.42	.42	.72	.73	.47	.65	.65	.64	.72	.63	.71	.67	.32	.62	.42	.65	.60	.67	.55	.60	.91	.70	.72	.59	W
X	.66	.41	.38	.38	.65	.72	.45	.75	.79	.67	.76	.67	.37	.73	.31	.57	.38	.66	.61	.76	.51	.92	.72	.92	.62	.73	X
Y	.70	.58	.36	.34	.69	.70	.46	.66	.74	.68	.77	.72	.61	.65	.25	.59	.36	.61	.65	.78	.50	.68	.74	.71	.92	.61	Y
Z	.52	.68	.53	.52	.70	.58	.56	.75	.80	.62	.64	.67	.59	.68	.48	.51	.50	.59	.62	.74	.53	.50	.66	.73	.64	.91	Z

rectangular grid (in this correspondence called a shape matrix) by polar quantization of the shape. It was shown that if the quantization parameters are selected properly, it is possible to reconstruct an original shape from its shape matrix. The transformation from a shape to a shape matrix was normalized so that independent of a shape's position, orientation, or scale, we obtain the same representation.

An alternative to polar quantization is the logarithmic polar quantization known as the logarithmic spirals [14]. In the logarithmic spirals, instead of taking a constant radial quantization step, the radial quantization step is increased logarithmically with the distance of points to the center of the grid. Polar quantization shares some of the same properties of logarithmic spirals such as producing shape description independent of a shape's orientation or scale. Polar quantization has the advantage of being simpler to implement and faster to compute than the logarithmic spirals.

Compared to shape signatures, shape matrices provide faster speed in discriminating shapes, and if the shapes under consideration are not too large ($L \leq 16$), they consume about the same amount of memory. For larger shapes, shape matrices consume more memory than shape signatures, however, shape matrices store information about holes in the shape while shape signatures are not capable of doing so. In terms of description and discrimination of

shapes, for simply connected objects whose radii intersect the boundary only once, shape matrices and shape signatures are logically equivalent. But for objects with holes or multiple intersections with the radii, shape matrices provide more information about a shape and are more accurate than shape signatures.

ACKNOWLEDGMENT

The author would like to thank Dr. C. Page and Dr. G. Stockman of the Department of Computer Science, Michigan State University, East Lansing, for their many helpful discussions and suggestions on this work. The help of J. Spanyer in the preparation of this correspondence is also appreciated.

REFERENCES

- [1] F. Atteneave, "Physical determinations of the judged complexity of shapes," *J. Exp. Psychol.*, vol. 53, no. 4, pp. 221-227, Apr. 1957.
- [2] D. R. Brown and D. H. Owen, "The metrics of visual form: Methodological dyspepsia," *Psychol. Bull.*, vol. 68, no. 4, pp. 243-250, 1976.
- [3] R. O. Duda and P. E. Hart, *Pattern Classification and Scene Analysis*. New York: Wiley, 1973.

- [4] S. A. Dudani, K. J. Breedy, and R. B. McGhee, "Aircraft classification by the moment invariants," *IEEE Trans. Comput.*, vol. C-26, pp. 39-46, 1977.
- [5] H. Freeman, "Shape discrimination via the use of critical points," *Pattern Recogn.*, vol. 10, pp. 159-166, 1978.
- [6] K.-S. Fu, *Syntactic Pattern Recognition and Application*. Englewood Cliffs, NJ: Prentice-Hall, 1982, pp. 79-128.
- [7] A. Goshtasby, "Template matching in rotated images," *IEEE Trans. Pattern Anal. Machine Intell.*, vol. PAMI-7, pp. 338-344, May 1985.
- [8] M.-K. Hu, "Visual pattern recognition by moment invariants," *IRE Trans. Inform. Theory*, pp. 179-187, 1962.
- [9] D. Marr and H. K. Nishihara, "Representation and recognition of the spatial organization of three-dimensional shapes," in *Proc. Roy. Soc. London, B.*, vol. 200, pp. 269-294, 1978.
- [10] T. Pavlidis, "A review of algorithms for shape analysis," *Comput. Graph. Image Processing*, vol. 7, pp. 243-258, 1978.
- [11] —, "Algorithms for shape analysis of contours and waveforms," *IEEE Trans. Pattern Anal. Machine Intell.*, vol. PAMI-2, pp. 301-312, July 1980.
- [12] T. Peli, "An algorithm for recognition and localization of rotated and scaled objects," *Proc. IEEE*, vol. 69, no. 4, pp. 483-485, 1981.
- [13] T. P. Wallace and P. A. Wintz, "An efficient three-dimensional aircraft recognition algorithm using normalized Fourier descriptors," *Comput. Graph. Image Processing*, vol. 13, pp. 99-125, 1980.
- [14] C. F. Weiman and G. Chaikin, "Logarithmic spiral grids for image processing and display," *Comput. Graph. Image Processing*, vol. 11, pp. 197-226, 1979.
- [15] C. T. Zahn and R. Z. Roskies, "Fourier descriptors for plane closed curves," *IEEE Trans. Comput.*, vol. C-21, pp. 269-281, Mar. 1972.
- [16] L. Zusne, *Visual Perception of Form*. New York: Academic, 1970, pp. 206-211.

A Cognitive Heuristic Algorithm for Reseau Mark Detection by Hill Climbing

B. V. SHEELA

Abstract—A hill-climbing approach for the automatic detection of Reseau marks (RM) on the vidicon type of imagery is presented. This procedure is based on the minimization of a figure of merit which is a measure of the clustering nature of the gray values of the Reseau pixels around a nominal value. The often-encountered problem of false detection is circumvented by incorporating the concept of "learning" the mean gray value of the RM pixels. Results of applying the algorithm to both synthetic and actual imagery demonstrate the efficacy of the proposed method.

Index Terms—Clustering, geometric distortions, hill-climbing, random search, remotely sensed imagery, Reseau marks, shadow casting, variable transformations, vidicon sensors.

I. INTRODUCTION

The concept of digital correction of remotely sensed imagery has been gaining acceptance around the world thanks to the development of very efficient and sophisticated image processing algorithms and the digital hardware to match them. The geometric errors in the vidicon type of imageries that are sensor related, termed the internal errors, could be characterized by the knowledge of the nominal and actual locations of the Reseau marks (RM). These marks are opaque cruciform shapes inscribed on the faceplate of the sensor whose locations on the imagery are to be accurately determined. A single scene/picture frame could contain as many as

Manuscript received February 2, 1983; revised November 28, 1983.

The author is with the ISRO Satellite Center, Mission Operating and Planning Division, Peenya Industrial Estate, Peenya, Bangalore-560-058, India.

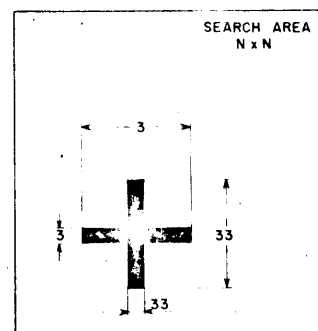


Fig. 1. Reseau mark inscribed in a search area.

81 (as in the case of the return beam vidicon [RBV] imagery of LANDSAT) uniformly spaced RM's. Typical dimensions of these marks would be 32-33 pixels along the arms and 3-4 pixels across (Fig. 1). The percentage uncertainty of the sensor dictates the area of the picture in which a particular RM could be found with certainty. This defines the so-called search area in which an RM is to be detected. Essentially, the problem with RM location is to determine the line number l_c and pixel number p_c of the center of the RM given the gray values $g_{i,j}$ of each of the pixels in the search area. As observed in [1], even a ± 1 percent geometric error leads to an uncertainty of 40 pixels in both horizontal and vertical directions around the nominal locations of the RM in RBV imagery. This makes search area dimensions as large as 128×128 pixels an inevitable necessity in order that the RM be found in the search area with certainty. One of the widely used methods for RM location is that of shadow casting [1], [2]. As observed by Bernstein in [2], this procedure suffers from a few disadvantages in that it is found to be too sensitive to the deviations in the size, shape, and intensity of RM's in addition to being incapable of recognizing the absence of a RM in a given search area. To overcome these pitfalls Bernstein has reported a new algorithm which takes advantage of the fact that RM's are invariably the darkest objects in the search area. Steps are also incorporated in that algorithm to discard fictitious RM's. This elegant method, based on local averaging, is admittedly very efficient and foolproof more often than not, but it is neither very difficult to envisage nor improbable to encounter situations where such a seemingly universal method could fail to detect a RM or could make a costlier mistake of false RM detection. This problem is addressed in Section II. Section III describes the new algorithm, while Section IV presents some test results followed by conclusions in Section V.

II. EARLIER METHODS FOR DETECTION

The only available method in the literature for RM detection had been that of Bernstein and his co-workers at the IBM corporation [1], [2], based on the "shadow-casting" procedure. In this method, the individual row and column sums of pixel gray levels in the search area are calculated and the detection is carried out by fitting a quadratic to these sums. This algorithm, which was reported to have worked well with simulated data, has been found to have failed to locate nearly 90 percent of the RM's in real RBV images. This failure was attributed to the deviations in the size, shape and intensity of RM's caused by beam distortions. To overcome this, Bernstein [2] has described an algorithm exploiting the fact that RM's, in spite of the variations in their parameters, are invariably the darkest objects in the search area. This algorithm finds the lowest column sum and tentatively calls this the column center of the RM. All columns around this whose sums are lower than the average of the lowest sum and its background are classified as Reseau columns. The middle column of these is deemed to be the center col-